Published in Colloids Surf. B 54, 160-164 (2007)

Synchrotron SAX and WAX diffraction study of a hydrated very long-chain, dendriditic amphiphile+DPPC mixture

Janka Karlovská[a], André A. Williams[b], Richard V. Macri[b], Richard D. Gandour[b], Sérgio S. Funari[c], Daniela Uhríková[a], Pavol Balgavý[a*]

[a]*Department of Physical Chemistry of Drugs, Faculty of Pharmacy, Comenius University, Odbojárov 10, 832 32 Bratislava, Slovakia*

[b]*Department of Chemistry MC 0212, Virginia Tech, Blacksburg, VA 24061, USA*

[c]*HASYLAB DESY, D-22603 Hamburg, Germany*

[*] Corresponding author. Fax: +421-50117-100.

E-mail address: pavol.balgavy@fpharm.uniba.sk

Abstract

The tri-headed anionic dendritic amphiphile, 4-(2-carboxyethyl)-4-[(icosyloxycarbonyl)amino]heptanedioic acid (3CCb20), forms solid-like gel-state mixed micelles with dipalmitoylphosphatidylcholine (DPPC) in excess water at 3CCb20 : DPPC = 0.91 : 1 molar ratio. On heating, these micelles transform into fluid bilayers stacked in the liquid crystalline lamellar L_α phase at about 40 °C. This phase transition and the microstructure of 3CCb20 + DPPC aggregates were studied using small- and wide-angle synchrotron X-ray diffraction. The ability of 3CCb20 to solubilize solid-like lipid bilayers could be important in microbiocidal activities of 3CCb20, including in its anti-HIV activity.

Keywords: amphiphiles; DPPC; micelles; bilayers; X-ray diffraction; phase transition

1. Introduction

Saturated fatty acids have a long history as microbicides against many pathogens [1-5]. Measurements of inhibitory activities can be problematic because of the very low solubility of saturated fatty acids in aqueous solutions [6]. Furthermore, as the chain length increases to C_{18} and beyond, the aqueous solubility becomes immeasurable. Knowing that the compounds completely dissolve in aqueous media enables speculation about how chain length affects microbiological activity. In a homologous series of compounds, antimicrobial activity can show a cut-off effect [7]. Without knowing that the amphiphiles fully dissolve in aqueous media, we cannot conclude that the cut-off effect is due to the "intrinsic" activity of the amphiphiles or due to the decreased solubility of the amphiphile in the microbiological media.

To overcome the challenge of low solubilities of saturated long-chain fatty acids, we have made very long-chain dendritic amphiphiles that are water soluble to 20 mM and show antimicrobial activity, especially against *Candida albicans*, *Mycobacterium smegmatis*, and *Saccharomyces cerevisiae* [8], and anti-HIV activity [Doncel, Macri, Williams, Sugandhi, and Gandour, unpublished]. One series of these novel tri-headed anionic amphiphiles,

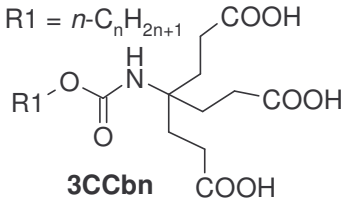

4-[(alkoxycarbonyl)amino]-4-(2-carboxyethyl)heptanedioic acids, (abbreviation 3CCbn, n = 14–22 is the number of carbon atoms in the alkyl substituent) is constructed from the Newkome-type dendrons [9] and is a new entry into the area of multi-headed amphiphiles. Multi-headed amphiphiles date back to the 1950s with the alkyl malonates [10] and the alkane-1,1,2-tricarboxylic acids [11]. Metal-chelating amphiphiles, derivatives [12] and analogues [13-16] of EDTA, have four carboxylates. Several amphiphiles based on aurintricarboxylic acid [17] and several amphiphilic polymers with dendritic anionic head groups [18] have good anti-HIV activity. The dendritic head-group structure and the very long chain of 3CCbn amphiphiles will impart properties different from those of natural saturated fatty acids.

The antimicrobial data for 3CCbn show that longer chains (3CCb18–22) are more active than the shorter chains (3CCb14–16). These data contrast with those of saturated fatty acids, where the most active compounds are in the range of C_8 to C_{14} [1-5]. A dendritic structure should reduce the absorption of an amphiphile into a cell. The highly branched structure of the head group resembles the dendritic structure of glycolipids that are anchored on the outside of cells. Branching and the triple charge might retard diffusion across membranes. Given the success of very long chain amphiphiles as antimicrobials, there might be a preference for absorption of these amphiphiles on pathogens as opposed to epithelial cells resulting in the reduced irritancy.

To understand molecular mechanisms in the biological activities of these compounds, their interactions with different cell constituents must be studied. Several researchers [2,5,19] have proposed that the microbicidal mechanism of action involves fatty acids interacting with membranes. Because of the long alkyl chains, 3CCbn will likely partition into biological membranes. Upon doing so, these amphiphiles will affect the structure and dynamics of the membrane. The phospholipid bilayer comprises the structural matrix of biological membranes. Understanding how amphiphiles interact with a phopholipid bilayer will provide clues to the molecular mechanism of the biological activity [7].

In this paper, we report the interaction of 3CCb20, a representative of a very long chain amphiphile, with model bilayers prepared from dipalmitoylphosphatidylcholine (DPPC) using small- (SAX) and wide-angle (WAX) synchrotron X-ray diffraction.

1. Materials and Methods

DPPC was purchased from Avanti Polar Lipids (Alabaster, USA). 3CCb20 was prepared from the Newkome-type dendrons [9] as described in [8]. 3CCb20 amphiphile and DPPC were mixed at 0.91 : 1 molar ratio in methanol+chloroform, the solvent was evaporated under a stream of gaseous nitrogen and its traces removed by an oil vacuum pump. Redistilled water was added at the H_2O : DPPC = 5 : 1 weight ratio and the mixture was homogenized mechanically. About 2 – 3 h before measurements, the mixture in the sample holder was heated to ~ 70 °C and cooled to room temperature twice. SAXD and WAXD experiments were performed at beamline A2 in HASYLAB at DESY using a monochromatic radiation of wavelength 0.15 nm [20]. The evacuated double-focusing camera was equipped with two linear delay line readout detectors [21,22]. The SAX detector was calibrated using rattail tendon

[23] and the WAX detector by tripalmitin [24,25]. Data reduction and normalization were done with the programs STAFO and OTOKO [26]. During temperature scans, the samples were heated from 20 to 80 °C in 60 min and the diffractograms were recorded for 10 s every min. The diffraction peaks were fitted with Lorentzians and positions of maxima, intensities, integral intensities and half widths of peaks at one half of their intensity were determined with a non-linear least-squares program. The cross-sectional area A of aliphatic chain was calculated from the position of WAX peak as in [27].

3. Results and Discussion

It is well known that DPPC forms lyotropic lamellar phases in excess water. On heating, the phase behaviour of the DPPC-H_2O system can be described in the form $L_c \rightarrow L_{\beta'} \rightarrow P_\beta \rightarrow L_\alpha$, where the three solid-like phases L_c, $L_{\beta'}$ and $P_{\beta'}$ have extended acyl chains predominantly in a *trans* configuration, while the lamellar fluid phase L_α has disordered acyl chains due to *trans* - *gauche* isomerization [27]. The L_c phase forms only if the DPPC - H_2O system has been annealed at low temperatures for an extended period of time [28-30]. In the $L_{\beta'}$ phase, the acyl chains are tilted to the bilayer normal, but become perpendicular to the bilayer plane in the P_β phase; the lamellae surface of the P_β phase is rippled [27]. Typical SAX and WAX diffractograms obtained for $L_{\beta'}$, P_β and L_α phases in fully hydrated DPPC are shown in Fig. 1; they agree with those in the literature [27]. The pretransition ($L_{\beta'} \rightarrow P_\beta$) and the main gel-liquid crystal phase transition ($P_{\beta'} \rightarrow L_\alpha$) estimated from temperature dependencies of several diffraction peak parameters were ~ 36 ± 1 °C and ~42 ± 1 °C, coinciding within experimental error with 35.48 ± 0.20 °C and 41.53 ± 0.02 °C, which were determined by scanning calorimetry at heating rate of 0.25 °C/min in [31].

For the 3CCb20+DPPC mixture, a broad SAX scattering distribution centered at $s = (0.15 - 0.20)\ nm^{-1}$ was observed at temperatures below 40 °C (Fig. 2). Up to this temperature, a strong WAX diffraction peak was observed at $s = (0.42 - 0.43)^{-1}\ nm^{-1}$ (Fig. 2). In the range 20 – 38 °C, the position of a broad SAX peak oscillated between $s = 0.15$ and $s = 0.20\ nm^{-1}$; the WAX peak shifted continuously from $s = 2.36\ nm^{-1}$ to $s = 2.32\ nm^{-1}$ (Fig. 3). The position of the WAX peak is typical for ordered aliphatic chains of gel-phase phospholipids [27]. The simultaneous absence of long-range ordering and presence of short-range ordering observed in the 3CCb20+DPPC mixture indicates the formation of mixed amphiphiles–phospholipid aggregates, possibly solid-like gel-state discoidal mixed micelles, as

in fully hydrated $C_{12}E_8$+DPPC and $C_{12}E_8$+DMPC mixtures [32]. Between 20 and 40 °C, a small SAX reflection (labelled a in Fig. 2) at $s_a \sim 0.1$ nm^{-1} indicates the formation of long-range order in the 3CCb20+DPPC mixture. Between 39 and 41 °C, the intensity of WAX reflection decreases; the WAX peak broadens and shifts to s ~ 2.18 - 2.17 nm^{-1} (Figs. 2 and 3). These changes indicate the disordering of aliphatic chains—the chain melting in the hydrophobic core of micelles. Simultaneously with this melting, the small SAX reflection at s ~ 0.1 nm^{-1} disappears; the integral intensity of the broad SAX reflection at s = (0.15 - 0.20) nm^{-1} decreases; two new peaks (labelled b and c in Fig. 2) appear. The ratio of positions of these two peaks remains constant $s_c : s_b = 2.00 \pm 0.01$ up to 80 °C. The appearance of these two peaks and their relative positions indicate that the chain-melting phase transition proceeds simultaneously with the micelle–lamellar phase transition. Finally, a small SAX peak (labelled d in Fig. 2) at s ~ 0.18 nm^{-1} is present between 60 and 80 °C. The temperature dependence of positions of SAX and WAX reflections is shown in Fig. 3. The gel-state micelle–fluid-state lamellar phase transition is reversible. During the rapid cooling from 80 to 20 °C in 5 min, the broad SAX reflection reappears (Fig. 2, top patterns at 20 °C).

From the positions of lamellar SAX reflections b and c as well as the position of the WAX reflection, we have calculated the repeat distance d of the lamellar phase and the cross-sectional area A of an aliphatic chain, respectively (Fig. 4). In comparison to DPPC, the repeat period d is larger in the fluid phase of the 3CCb20+DPPC mixture. Both the electrostatic repulsion of bilayers (charged negatively by 3CCb20) and the bilayer thickness increase (the aliphatic chain in 3CCb20 is longer than those in DPPC) can contribute to this effect. The cross-sectional area A is smaller in the gel-state micelles and fluid bilayers of 3CCb20+DPPC than in the gel-state and fluid bilayers of pure DPPC, respectively. This improved packing in the hydrophobic region can be caused by an increased chain–chain van der Waals attraction in the 3CCb20+DPPC mixture, because of the increase in the mean chain length.

Amphiphiles partition between the aqueous phase and phospholipid bilayers and, after reaching some critical amphiphile/phospholipid molar ratio in the bilayers, the mixed bilayers transform into mixed micelles; this transformation commonly denoted solubilization is widely known and used [33-36]. The transformation is driven by a very large difference in spontaneous curvatures between phospholipid and amphiphile which is dependent on the amphiphile/phospholipid molar ratio. Decreasing the amphiphile concentration—by the dissolution of mixed micelles [37-39] or by the reduction of partitioning of the amphiphile into a lipid

phase by changing the temperature [40-44]—results in a transformation into bilayer vesicles. For several homologous series of amphiphiles, short-chain homologues decrease and long-chain homologs increase the main phase transition temperature of DPPC when their chain length approaches or is longer than the acyl chain length of DPPC (see [45] for a review and discussion). By extending the van't Hoff theory of freezing point depression, one can show that the decrease and increase in phase transition temperature is connected with the surfactant partitioning into the lipid bilayer. The decrease occurs when the partition coefficient of an amphiphile between the fluid-state bilayer and the aqueous phase, K_L, is higher than the partition coefficient between the gel-state bilayer and the aqueous phase, K_G, while the increase occurs when $K_L/K_G<1$ [30,31,46,47]. The temperature induced gel state micelle – fluid bilayer observed in the present study could be caused by this partition effect in combination with the spontaneous curvature mechanism.

In summary, our results show that 3CCb20 integrates into the lipid bilayer of DPPC and, as a result, changes the phase behavior of DPPC. This unique amphiphile with a dendritic head and a single, very long chain (20 carbons) affects the phase behavior of DPPC differently than the saturated C_{12}-C_{20} fatty acids [48,49], which have a single carboxy as a head group. The hydrated tri-carboxyl head likely occupies a greater volume than a single hydrated carboxy. The increased volume should lead to a greater spacing of the amphiphiles in the bilayer and, due to the conical shape shape of the amphiphile, greater curvature as demonstrated by the formation of discoidal mixed micelles similar to those formed by fully hydrated $C_{12}E_8$+DPPC [32].

It is now established that biological membranes are highly sophisticated structures assembled of distinct lipid domains that functionally organize the proteins embedded in the lipid bilayer. One of these domain types, termed rafts, is in a solid-like ordered state [50]. The rafts are present in most mammalian plasma membranes and can serve as platforms for both signaling as well as the entry of pathogens such as viruses, including the HIV [50-55]. Also the lipid composition of native HIV membranes resembles raft domains [56]. The ability of 3CCb20 to solubilize ordered solid-like gel state bilayers could contribute in its anti HIV activity.

Acknowledgement

This work was supported by the European Community - Research Infrastructure Action under the FP6 "Structuring the European Research Area" Programme Contract RII3-CT-2004-506008 (HASYLAB project II-05-018 EC) and by the VEGA grant 1/0123/03 to DU. PB, RDG, AAW and DU thank the staff of HASYLAB for hospitality.

References

[1] J.E. Walker, J. Infect. Dis. 35 (1924) 557-566.

[2] C. Nieman, Bacteriol. Rev. 18 (1954) 147-163.

[3] J.J. Kabara, D.M. Swieczkowski, A.J. Conley, J.P. Truant, Antimicrob. Agents Chemother. 2 (1972) 23-28.

[4] E. Kondo, K. Kanai, Jpn. J. Med. Sci. Biol. 25 (1972) 1-13.

[5] H. Thormar, G. Bergsson, Recent Devel. Antiviral Res. 1 (2001) 157-173.

[6] H. Vorum, R. Brodersen, U. Kragh-Hansen, A.O. Pedersen, Biochim. Biophys. Acta 1126 (1992) 135-142.

[7] P. Balgavý, F. Devínsky, Adv. Colloid Interface Sci. 66 (1996) 23-63.

[8] A.A. Williams, E.W. Sugandhi, R.V. Macri, J.O. Falkinham, R.D. Gandour, Antimicrob. Agents Chemother. submitted (2006) .

[9] G.R. Newkome, C.D. Weis, G.R. Moorefield, B. Baker, J. Childs, J. Epperson, Angew. Chem. Int. Ed. Engl. 37 (1998) 307-310.

[10] K. Shinoda, J. Phys. Chem. 59 (1955) 432-435.

[11] K. Shinoda, J. Phys. Chem. 60 (1956) 1439-1441.

[12] K. Machajová, P. Butvin, J. Majer, Farm. Obzor 52 (1983) 43-50.

[13] S.C. Miller, F.W. Bruenger, G. Kuswik-Rabiega, R.D. Lloyd, Health Phys. 63 (1992) 195-197.

[14] L. Schmitt, C. Dietrich, R. Tampe, J. Am. Chem. Soc. 116 (1994) 8485-8491.

[15] M.V.D. Nguyen, M.E. Brik, B.N. Ouvrard, J. Courtieu, L. Nicolas, A. Gaudemer, Bull. Soc. Chim. Belg. 105 (1996) 181-183.

[16] K. Kimpe, T.N. Parac-Vogt, S. Laurent, C. Pierart, L. Vander Elst, R.N. Muller, K. Binnemans, Eur. J. Inorg. Chem. (2003) 3021-3027.

[17] M. Cushman, S. Insaf, G. Paul, J.A. Ruell, E. De Clercq, D. Schols, C. Pannecouque, M. Witvrouw, C.A. Schaeffer, J.A. Turpin, K. Williamson, W.G. Rice, J. Med. Chem. 42 (1999) 1767-1777.

[18] A. Leydet, C. Moullet, J.P. Roque, M. Witvrouw, C. Pannecouque, G. Andrei, R. Snoeck, J. Neyts, D. Schols, E. De Clercq, J. Med. Chem. 41 (1998) 4927-4932.

[19] K. Kanai, E. Kondo, Jpn. J. Med. Sci. Biol. 32 (1979) 135-174.

[20] Small Angle X-Ray Scattering @ Hasylab, DESY Hamburg. http://www-hasylab.desy.de/science/groups/saxs_group/welcome.htm, 2005.

[21] A. Gabriel, Rev. Sci. Instrum. 48 (1977) 1303-1305.

[22] G. Rapp, A. Gabriel, M. Dosire, M.H.J. Koch, Nucl. Instrum. Methods Phys. Res. A 375 (1995) 178-182.

[23] A. Bigi, N. Roveri, in: S. Ebashi, M. Koch, E. Rubenstein (Eds.), Handbook on Synchrotron Radiation, Vol. 4, Elsevier Science Publishers B.V., Amsterdam, 1991, pp. 199-239.

[24] D. Chapman, Chem. Rev. 62 (1962) 433-453.

[25] T.C. Huang, H. Toraya, T.N. Blanton, Y. Wu, J. Appl. Crystallogr. 26 (1993) 180-184.

[26] C. Boulin, R. Kempf, M.H.J. Koch, S.M. McLaughlin, Nucl. Instrum. Methods Phys. Res. A 249 (1986) 399-407.

[27] M.J. Ruocco, G. G. Shipley, Biochim. Biophys. Acta 684 (1982) 59-66.

[28] M.J. Ruocco, G.G. Shipley, Biochim. Biophys. Acta 691 (1982) 309-320.

[29] J. Gallová, P. Balgavý, FEBS Lett. 255 (1989) 354-357.

[30] J. Gallová, PhD. Thesis, Faculty of Pharmacy and Faculty of Mathematics and Physics, Comenius University, Bratislava, 1993.

[31] J. Gallová, Interaction of the homologous series of N-alkyl-N,N-dimethylamine N-oxides with the dipalmitoylphosphatidylcholine model membrane. DSC study. Final Report of the Project 27s9, Action Slovakia-Austria, Bratislava-Graz, 1999.

[32] S.S. Funari, B. Nuscher, G. Rapp, K. Beyer, Proc. Natl. Acad. Sci. USA 98 (2001) 8938-8943.

[33] D. Lichtenberg, Biochim. Biophys. Acta 821 (1985) 470-478.

[34] D. Lichtenberg, E. Opatowski, M.M. Kozlov, Biochim. Biophys. Acta 1508 (2000) 1-19.

[35] M. le Maire, P. Champeil, J.V. Moller, Biochim. Biophys. Acta 1508 (2000) 86-111.

[36] J. Rigaud, M. Chami, O. Lambert, D. Levy, J. Ranck, Biochim. Biophys. Acta 1508 (2000) 112-128.

[37] M. Ollivon, O. Eidelman, R. Blumenthal, A. Walter, Biochemistry 27 (1988) 1695-1703.

[38] M. Ollivon, S. Lesieur, C. Grabielle-Madelmont, M. Paternostre, Biochim. Biophys. Acta 1508 (2000) 34-50.

[39] B.H. Yue, C.Y. Huang, M.P. Nieh, C.J. Glinka, J. Katsaras, Journal of Physical Chemistry B 109 (2005) 609-616.

[40] A.I. Polozova, G.E. Dubachev, T.N. Simonova, L.I. Barsukov, FEBS Lett. 358 (1995) 17-22.

[41] A.N. Goltsov, L.I. Barsukov, J. Biol. Phys. 26 (2000) 27-41.

[42] P. Lesieur, M.A. Kiselev, L.I. Barsukov, D. Lombardo, J. Appl. Crystallogr. 33 (2000) 623-627.

[43] P.R. Majhi, A. Blume, J. Phys. Chem. B 106 (2002) 10753-10763.

[44] S. Keller, H. Heerklotz, N. Jahnke, A. Blume, Biophys. J. 90 (2006) 3750-3758.

[45] K. Lohner, Chem. Phys. Lipids 57 (1991) 341-362.

[46] J.M. Sturtevant, Proc. Natl. Acad. Sci. USA 81 (1984) 1398-1400.

[47] Y. Kaminoh, C. Tashiro, H. Kamaya, I. Ueda, Biochim. Biophys. Acta 946 (1988) 215-220.

[48] J.M. Seddon, R.H. Templer, N.A. Warrender, Z. Huang, G. Cevc, D. Marsh, Biochim. Biophys. 1327 (1997) 131-147.

[49] R. Koynova, B. Tenchov, Curr. Opin. Colloid Interface Sci. 6 (2001) 277-286.

[50] J. Fantini, N. Garmy, R. Mahfoud, N. Yahi, Expert Rev. Mol. Med. 2002 (2002) 1-22.

[51] S. Manes, G. del Real, R.A. Lacalle, P. Lucas, C. Gomez-Mouton, S. Sanchez-Palomino, R. Delgado, J. Alcami, E. Mira, A. Martinez, EMBO Rep. 1 (2000) 190-196.

[52] S. Manes, G. del Real, A. Martinez, Nat. Rev. Immunol. 3 (2003) 557-568.

[53] S.S. Rawat, B.T. Johnson, A. Puri, Biosci. Rep. 25 (2005) 329-343.

[54] G.F. Doncel, Hum. Reprod. Update 12 (2006) 103-117.

[55] K.I. Lim, J. Yin, Biotechnol. Bioeng. 93 (2006) 246-257.

[56] B. Brugger, B. Glass, P. Haberkant, I. Leibrecht, F.T. Wieland, H.G. Krausslich, Proc. Natl. Acad. Sci. USA 103 (2006) 2641-2646.

Figure legends

Fig. 1. SAX and WAX diffraction patterns of $L_{\beta'}$(20 °C), P_{β} (38 °C) and L_{α} (43 °C) phases in hydrated DPPC.

Fig. 2. SAX and WAX diffraction patterns of hydrated DPPC+3CCb20 mixture.

Fig. 3. Temperature dependence of positions of SAX and WAX reflections in the hydrated DPPC+3CCb20 mixture. For reflections a, b, c and d see Fig. 1.

Fig. 4 Temperature dependence of the lattice parameters and cross section area A of aliphatic chains of hydrated DPPC (♦) and DPPC+3CCb20 mixture (●).

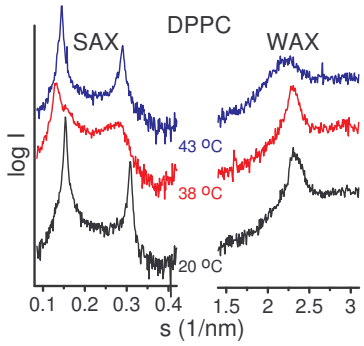

Fig. 1 SAX and WAX diffraction patterns of $L_{\beta'}$(20 °C), P_{β} (38 °C) and L_{α} (43 °C) phases in DPPC.

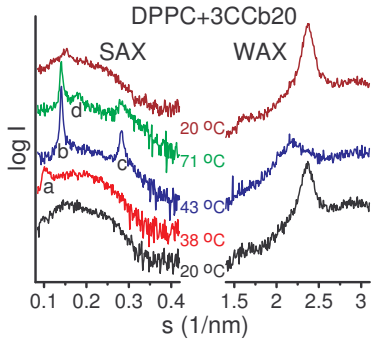

Fig. 2 SAX and WAX diffraction patterns of hydrated DPPC+3CCb20 mixture.

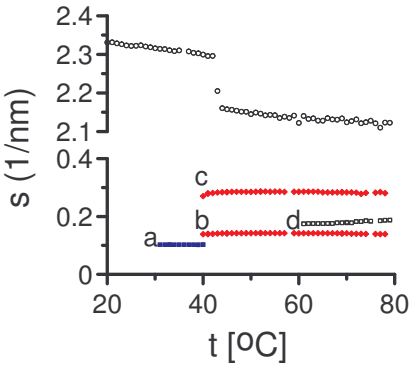

Fig. 3 Temperature dependence of positions of SAX and WAX reflections in the DPPC+3CCb20 mixture. For reflections a, b, c and d see Fig. 1.

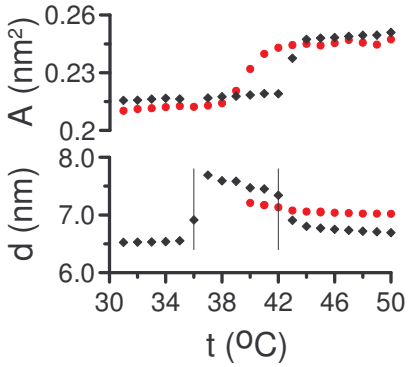

Fig. 4 Temperature dependence of lattice parameters of DPPC (♦) and DPPC+3CCb20 mixture (●).